IAC-22-A6.1.3

Lightcurve Generation Using Neuromorphic Event-Based Sensors

A. Jolley[a]*, J. Rodriguez[b], T. Schildknecht[b], A. Marcireau[a], G. Cohen[a]

[a] *International Centre for Neuromorphic Systems, Western Sydney University, Great Western Highway, Werrington, NSW, Australia, a.jolley@westernsydney.edu.au*
[b] *Astronomical Institute University of Bern (AIUB), Sidlerstrasse 5, 3012 Bern , Switzerland*
* Corresponding Author

Abstract

Frame-based optical sensors have been used for many years to produce lightcurves of space objects, from which information about those objects may be inferred. A relatively new type of optical sensor, known as a neuromorphic, or event-based, sensor is gaining attention as a promising tool for space object detection and characterisation. Comprising an array of pixels that function entirely independently and asynchronously, event-based sensors operate with microsecond temporal resolution, high dynamic range, and often with far lower data rates than frame-based sensors. An event-based pixel only outputs data when there is a change of brightness incident on that pixel that exceeds adjustable thresholds. We used a Prophesee Gen 4 EM event-based sensor that outputs not only the time of each detected change in brightness, but also a time-encoded value proportional to the brightness at the pixel after the change, to produce lightcurves of five satellites. The temporal resolution of the lightcurves that we produced varied from object to object, but in all cases there were many data points per second. Furthermore, since the event-based sensor operates without a shutter or set exposure interval, sudden or short duration brightness changes that would otherwise be missed during frame readout or smoothed by the effect of an exposure interval are captured. The results demonstrate that event-based sensors have considerable potential as space situational awareness tools.

Keywords: Event-Based Sensor, Neuromorphic, Space Domain Awareness, Lightcurve, Satellite Characterisation

Acronyms/Abbreviations

ADU – Analog to digital unit
CCD – Charge coupled device
CMOS – Complementary metal oxide semiconductor
EBS – Event-based sensor
EM – Exposure measurement
FoV – Field of view
LEO – Low Earth Orbit
SDA – Space Domain Awareness
TCDS – Time-Domain Correlated Double Sampling

1. Introduction

For many years, researchers have been measuring the brightness of satellites for the purpose of characterisation [1,2]. Taking repeated measurements over a single satellite pass and plotting those measurements against time produces a satellite 'lightcurve', which can then be analysed to derive more information regarding that satellite than a few sparse measurements can provide. As space-based services have become increasingly important to maintaining our way of life, with a corresponding increase in congestion in orbit, the need for satellites characterisation information has also increased.

Usually, satellites appear as point sources, and inferring characterisation information from brightness measurements is not trivial. Maximising the amount of information that can be derived requires high temporal resolution and dynamic range so that fast, short duration changes are not missed and to avoid saturation or underexposure effects. Previous studies have shown that using lightcurves for satellite surface material identification might be more successful if the lightcurves' temporal resolution is greater than what is commonly produced with conventional optical sensors [3,4].

Neuromorphic, or event-based, sensors (EBSs) are attracting attention for their potential for use for space domain awareness (SDA) applications, including satellite characterisation [5,6]. Event-based sensors are based on a pixel array, much like charge coupled device (CCD) or complementary metal oxide semiconductor (CMOS) sensors, however circuitry built into each pixel allows all pixels in the array to operate independently of each other. A given pixel only outputs data, known as events, when that pixel detects changes in brightness above or below user-selectable internal contrast thresholds. An increase in brightness is known as an 'ON' event, and a decrease in brightness is known as an 'OFF' event. Events are recorded as they occur, with microsecond temporal resolution, rather than at arbitrarily determined frame readout rates. The circuitry in each pixel, which detects changes in log-luminance, results in very high dynamic range, often in excess of 120 dB, and as high as 143 dB [7].

Some EBS models have additional circuitry in each pixel that measures absolute brightness levels [8]. These

time-domain correlated double sampling (TCDS) exposure measurements (EMs) are triggered by ON and OFF events, and therefore are also asynchronous. Further, rather than relying on a fixed, pre-defined exposure time, the exposure measurement is conducted by measuring the time taken for the pixel's photodiode voltage to drop from a high threshold value to a low threshold value. The discharge rate is proportional to the photocurrent, and therefore the EM value is taken to be the inverse of the time taken for the voltage drop to occur. Exposure measurements are as sparse as change detection events because only the pixel that detected a change event conducts an exposure measurement. As a result, event-based sensor data rates are often orders of magnitude smaller than similar temporal length high-speed frame-based recordings.

Our team at Western Sydney University and the University of Bern conducted an experiment on 6th July 2022 with a 4th generation EM EBS from Prophesee [9] and an ANDOR Neo 5.5 sCMOS camera to determine whether EBSs might offer advantages over traditional frame-based sensors for lightcurve production. Five satellite lightcurves were generated with the EBS. Unfortunately, due to technical problems with one of the telescope mounts, CMOS data were only able to be acquired simultaneously for one of those satellites. Nonetheless, the CMOS data offered an important point of comparison to the EBS data. The results demonstrate that EBSs can perform well at producing lightcurves of bright satellites, however further work is required to enable their use with fainter satellites.

2. Experiment setup and method

The experiment was conducted at the University of Bern's Zimmerwald observatory in Switzerland [10], depicted at Fig. 1, utilising both the 0.8 m ZimMain telescope and one of the dual 0.4 m ZimTwin telescopes. The CMOS camera was fitted to the 0.8 m ZimMain telescope, both of which were controlled on-site, and the EBS was fitted to one of the two twin-mounted 40 cm ZimTwin telescopes. The ZimTwin telescope was also controlled on-site, however the EBS was connected to an Intel NUC computer, and controlled remotely from Australia using custom-developed software.

Target satellites were selected using the Heavens Above website [11] to search for bright satellite passes. Once a satellite had been selected, both telescopes were commanded to track the satellite, and recording was commenced for each sensor independently when the satellite was seen to be in the field of view (FoV); from on-site for the CMOS sensor, and from Australia for the EBS. EBS recording was stopped when the satellite was no longer visible above the horizon. Due to a technical problem, the ZimMain telescope was rarely able to maintain tracking on satellites that moved across the sky

relatively quickly, and in these cases little to no CMOS data were able to be acquired.

Fig. 1. Zimmerwald Observatory near Bern, Switzerland.

The CMOS exposure time was set to 80 ms, and data were processed using the well-established, aperture photometry technique described in [12], including background subtraction, but without compensating for changing atmospheric extinction or calibrating by reference to standard stars. The resultant processed data are instrumental brightness, in analog-to-digital units (ADU).

2.1 Event-based sensor settings and data processing

Because the EBS does not output frames, a novel processing method is required for those data. The EBS output can be represented as a five-column stream of numbers: x-axis pixel location, y-axis pixel location, exposure, polarity, and time. Together, the x-axis and y-axis pixel location values indicate the pixel that is outputting data. Exposure is a binary value that indicates whether the output is related to an exposure measurement (1) or a brightness change event (0). Polarity is also a binary value. For brightness change events, a polarity value of 1 indicates an ON event, and a 0 indicates an OFF event. For exposure measurements, a polarity value of 1 indicates the crossing of the upper EM threshold, and 0 indicates the crossing of the lower EM threshold. Time is an unsigned 64-bit value indicating the number of microseconds since the start of the internal EBS clock for that recording.

A custom program was written to process the EBS data, event-by-event, rather than grouping the data into discrete time intervals as with frame-based data. This was important for maintaining the temporal resolution of the data. The program is based on a custom object tracker that detects objects in the FoV and classifies them as either stars or satellites based on the motion across the pixel array. The satellite of interest is assumed to be close to stationary in the FoV. Each event or EM that occurs is either associated with the satellite or a star, or is assessed to be noise, based on its distance

from the centre of each object in the FoV. Every time an EM is associated with the satellite of interest, the EM value for that pixel is recorded, and all EM values within a user-defined radius of the centre of the satellite are summed. The result of the summation is the brightness of the satellite at the time of the latest EM. The satellite's lightcurve is then created by plotting those brightness measurements versus time.

Figure 2 is a frame from a video rendering of one of the recordings. In the video rendering, events are indicated by yellow pixels, which gradually fade over a short period of time. Three stars are visible as yellow streaks because they are moving across the pixel array, with a green circle around the centre of each star. The satellite, which is being tracked by the telescope, is labelled and circled cyan.
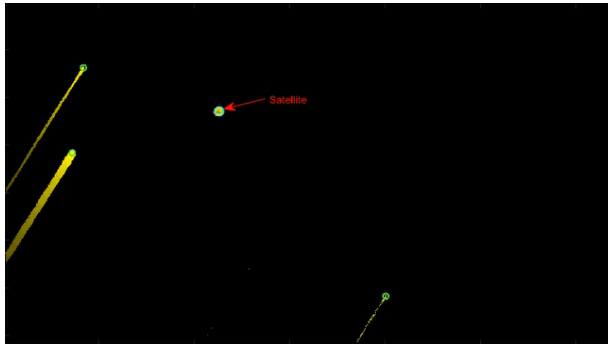

Fig. 2. Frame from a video rendering of EBS recording.

However, there is one major complicating factor in particular that adds complexity to lightcurve generation when using an EBS. Pixel exposure measurements are triggered by change detection events, however they are not completed instantaneously; rather they take a finite time, and the time required is inversely proportional to the log illuminance incident on that pixel. If a pixel is in the process of conducting an exposure measurement, and then it experiences a new change detection event, that event will interrupt the exposure measurement, which will be lost, and a new exposure measurement will be initiated. If a pixel is exposed to a rapid, large magnitude change in brightness, it is possible for several exposure measurements in a row to be interrupted by successive change detection events, with only the final exposure measurements being recorded once the rate of change of brightness had sufficiently subsided. Thus, if the brightness changes too rapidly, many exposure measurements could be lost. Although changes in satellite brightness do generate events, by far the most significant source of events for a satellite being held stationary in the FoV is atmospheric turbulence. Scintillation, which occurs when light passes through Earth's turbulent atmosphere, is the reason that stars twinkle, and it causes light from a satellite to move quickly and seemingly randomly about a cluster of

pixels in the EBS array, constantly generating events. Without atmospheric effects, a constant-brightness satellite that remains stationary in an EBS pixel array will not generate any events or exposure measurements, and will seem to disappear. In our experience, however, even a constant light source can generate hundreds or thousands of events per second, depending upon its brightness. The brighter an object is, the more events per second it will generate, and thus a high event-rate is possible even if the satellite is not changing in brightness. However, because exposure measurement integration times are inversely proportional to brightness, a higher event-rate associated with a brighter object does not necessarily result in an increased rate of interrupted exposure measurements because the exposure measurements are completed more quickly. Conversely, an object that is sufficiently faint will rarely or never exceed the internal EBS pixel contrast thresholds, and thus generate very few events and associated exposure measurements. It is for this reason that bright satellites were selected for this experiment.

An EBS's output can be modulated by adjusting various internal sensor settings, known as 'biases'. 20 different biases are available to be adjusted for the EBS model used in this experiment. Many of the biases are interdependent, such that adjusting one bias will impact the effect of several other biases, considerably complicating any effort to find an optimal set of bias settings for any particular task. Regardless, there are five main biases that were adjusted to control the EBS's output for the purpose of this experiment, each of which has a range of possible values from 0 to 255. Their primary effects, and their settings during this experiment are:

- Bias_diff_on. This bias controls the sensitivity of pixels to increases in brightness. Reducing its value will reduce the relative increase in brightness that pixels will need to experience for ON events to be generated, and therefore more ON events should be expected to be output per unit of time. Increasing the bias value will have the opposite effect. This bias was set to 150.
- Bias_diff_off. The primary function of this bias is similar to Bias_diff_on, except that it controls sensitivity to reductions in brightness. Increasing its value will reduce the relative decrease in brightness that pixels will need to experience for OFF events to be generated, and therefore more OFF events should be expected to be output per unit of time. Decreasing its value will have the opposite effect. This bias was set to 23.
- Vref_H. This bias sets the integration start point for exposure measurements. Its value was set to 250.

- Vref_L. This bias sets the integration end point for exposure measurements. Setting this bias to a lower value (further from Vref_H) increases the exposure measurement integration time, but also reduces the measurement error. A higher value will shorten the integration time, reducing the probability of measurements being interrupted by new events, but also increasing measurement error. This bias was set to 150.
- Bias_refr. This bias controls the refractory period; an intentional pixel dead time that prevents a pixel from outputting any events for a certain length of time after an event. A longer refractory period will increase the probability of brightness change events being missed, however it will also prevent an exposure measurement being interrupted by a new event during the dead time. This bias was set to 128.

Because the sensors were presumably not designed with our purpose in mind, we discovered that the standard settings were not suitable for lightcurve generation, and that almost no exposure measurements were output, even for very bright satellites. Many nights of experimentation were conducted prior to this study to find suitable settings for the aforementioned, and other, biases for the purpose of satellite lightcurve generation. A combination of reduction in change detection sensitivity, increase in EM integration time, and increased refractory period compared to standard settings was found to produce many exposure measurements per second for bright objects. However, objects fainter than approximately magnitude 8 were still not able to produce sufficient exposure measurements for lightcurve generation, hence we specifically selected bright satellites for this experiment. The number of possible EBS bias combinations is prohibitively large to find optimum settings by trial and error, however it is likely that performance against fainter satellites can be improved with further exploration of the effect of selecting different settings.

3. Results and discussion

In total, five Low Earth Orbit (LEO) satellites were observed with the EBS; three rocket bodies and two payloads, as indicated in Table 1.

Each of the satellites exhibited a steady increase in brightness as they ascended in the sky, followed by a steady decrease in brightness as they descended towards the other horizon, which is as expected because of the reduced atmospheric extinction for a satellite that is higher in the sky. This was particularly true for the rocket bodies, which lack complex structure that might otherwise cause glints or dips in brightness. The four non-stabilised satellite lightcurves are depicted in Fig. 3.
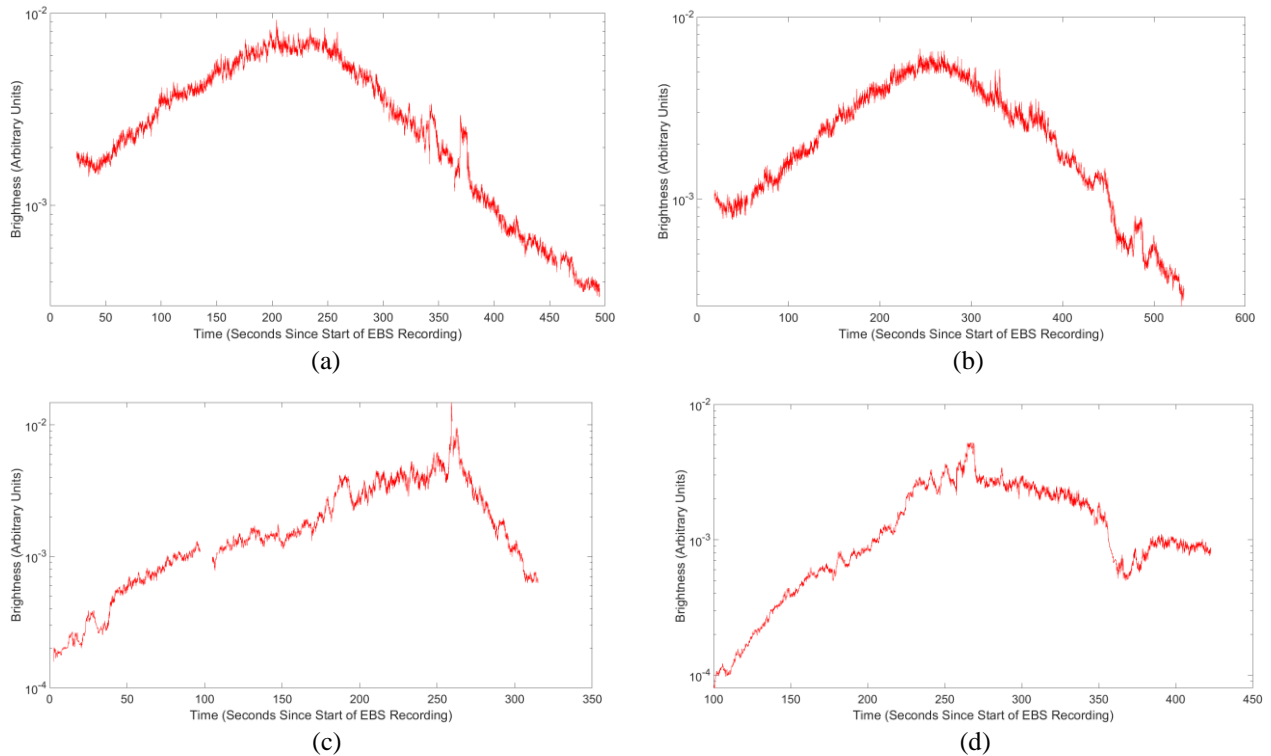

(a)

(b)

(c)

(d)

Fig. 3. Four of the five EBS lightcurves: SL-16 rocket bodies (a) and (b), an Ariane-40 rocket body (c), and the decommissioned Resurs DK-1 satellite (d).

Table 1. Satellites observed with the EBS.

Satellite	NORAD ID	Stabilised
SL-16 R/B	17590	No
SL-16 R/B	20625	No
Ariane 40 R/B	23608	No
Resurs DK-1	29228	No
Terra	25994	Yes

There was a clear correlation between satellite brightness and the number of exposure measurements per second, with the SL-16 rocket bodies averaging over 1250 data points per second, the Ariane 40 rocket body and Resurs DK-1 averaging approximately 800 data points per second, and Terra averaging over 1400. In all cases, there were fewer data per second when the satellites were fainter compared to when they were at their brightest. That is consistent with the authors' experience that brighter objects reliably generate more events than fainter objects; and since exposure measurements are triggered by events, we expect more lightcurve data for brighter objects. Despite the high temporal resolution of the data, the EBS file sizes ranged from merely 5.7 MB to 20.8 MB, with recordings between 300 s and 525 s in duration.

Data were acquired simultaneously with both the EBS and the CMOS sensor for the stabilised satellite, Terra. The lightcurve produced with the EBS, is at Fig. 4, and the lightcurve produced with the CMOS sensor is at Fig. 5. Only approximately 80 seconds of CMOS data were acquired because the 0.8 m ZimMain telescope was not able to maintain tracking on the satellite when the required telescope slew rate was highest.
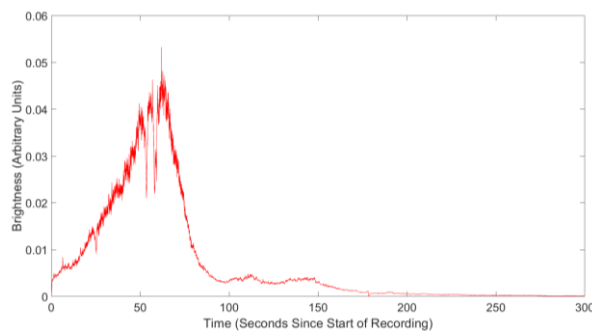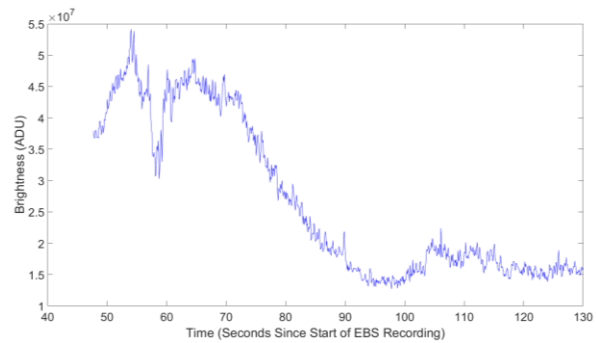

Fig. 4. EBS Terra lightcurve.

Fig. 5. CMOS Terra lightcurve.

To plot both the CMOS and EBS lightcurves on the same axes, the data needed to be scaled such that CMOS ADU values could be equated to EBS brightness values. The EBS pixel brightness measurements are on a scale that ranges from zero to one, whereas the 16-bit CMOS sensor outputs ADU values from zero to 65535 for each pixel. To reduce the discrepancy between the two scales, the CMOS lightcurve data were normalised to the maximum value. However, the CMOS sensor outputs pixel values on a linear scale, whereas the EBS measures log intensity. Raising the CMOS data values to the power of e should therefore be expected to result in a linear relationship between the CMOS and EBS data. But because the EBS data are unevenly spaced in time, both those and the CMOS data were first interpolated at common time steps, every 0.01 seconds, before they were compared.

Figure 6 is a plot of CMOS data versus EBS data scaled and interpolated as described. At lower light levels, it can be seen that there is indeed a linear relationship between the two datasets. The breakdown in linearity above about 0.02 on the x-axis can be explained by the fact that many of the CMOS pixels had saturated at higher brightness levels, causing the brightness to be under-recorded. A line was fit through all of the points below 0.02 on the x-axis, which can also be seen in Fig. 4. The coefficients of the linear fit describe how the data need to be adjusted so that they can be plotted on the same scale. In this case, the linear fit passed through the x-axis (EBS Data) at 0.0015, and had a slope of 19.3. Therefore, 0.0015 was subtracted from the EBS data, which were then multiplied by 19.3.
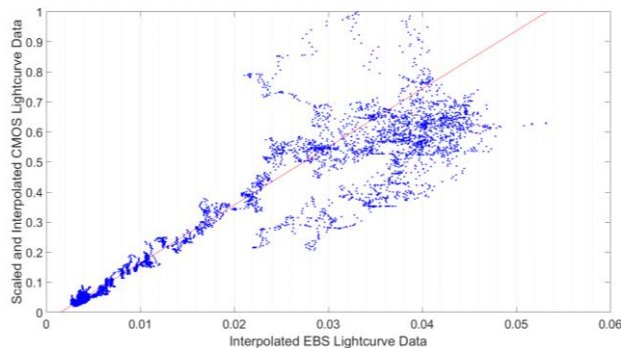
Fig. 6. CMOS brightness data versus EBS brightness
data for Terra, scaled for ease of comparison

Having appropriately scaled the data, Fig. 7 depicts the EBS and CMOS lightcurves plotted on the same axes. At lower brightness levels, beyond approximately 70 s on the x-axis, the data for the two sensors match very well. On visual inspection, the EBS data appear to exhibit slightly less variability than the CMOS data in this part of the plot, however more satellite observations are required to be able to determine whether the EBS data are less noisy, or whether the CMOS sensor is recording finer detail in the brightness fluctuations. At the brighter end of the plot, prior to approximately 70 s on the x-axis, the CMOS values are almost always lower than the EBS values. This could be explained by the fact that the CMOS sensor was considerably saturated when the satellite was bright, however between approximately 51 s and 55 s the CMOS lightcurve spikes well above the EBS lightcurve, which actually dips in brightness. As at the time of writing, there does not seem to be a clear explanation for that discrepancy.
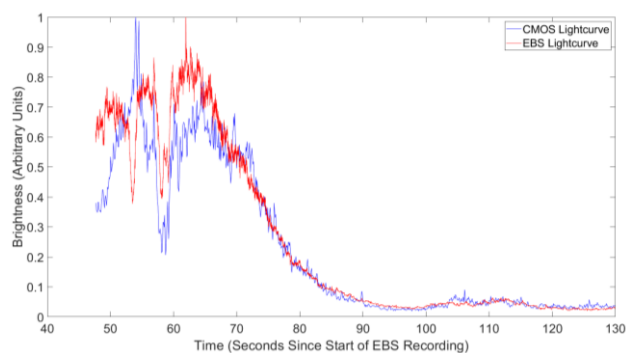

Fig. 7. CMOS and EBS lightcurves for Terra; data
adjusted to be on the same scale

4. Conclusion

This experiment, using a Prophesee Gen 4 EM event-based sensor, has demonstrated that event-based sensors can be used to generate high-temporal-resolution lightcurves of satellites. This opens the door

for new means of conducting SDA tasks because long recordings can be made and processed quickly without requiring the capture, storage and processing of large quantities of data. Current EBSs appear only able to accurately measure relatively bright satellites, however, although further investigation into optimum bias settings might improve the ability to measure faint satellites. In future, it is possible that EBS pixels could be designed specifically for SDA purposes, such as by preventing exposure measurements from being interrupted by new events mid-integration. New pixel designs might significantly improve performance for this application. Finally, as they are low size, weight and power, low data-rate sensors, EBSs could be well suited to space-based SDA.

References

[1] A. Chaudhary, T. Payne, S. Gregory, P. Dao, Fingerprinting of Non-Resolved Three-axis Stabilized Space Objects Using a Two-Facet Analytical Model, Proceedings of the 2011 AMOS Technical Conference, Kihei, Maui, HI, 2011, September.

[2] J.V. Lambert, K.E. Kissell, The Early Development of Satellite Characterization Capabilities at the Air Force Laboratories, Proceedings of the 2006 AMOS Technical Conference, Kihei, Maui, HI, 2006, September.

[3] A. Jolley, Multicolour Optical Photometry of Active Geostationary Satellites Using a Small Aperture Telescope, Master Thesis, Physics Dept., Royal Military College of Canada, Kingston, Ontario, 2014.

[4] H. Krantz, E.C. Pearce, L. Avner, K. Rockowitz, Chimera: a High-Speed Three-Color Photometer for Satellite Characterization, Proceedings of the 2018 AMOS Technical Conference, Kihei, Maui, HI, 2018, September.

[5] G. Cohen, S. Afshar, B. Morreale, T. Bessell, A. Wabnitz, M. Rutten, A. van Schaik, Event-Based Sensing for Space Situational Awareness, The Journal of the Astronautical Sciences, Vol. 66, pp. 125-141, 2019, https://doi.org/10.1007/s40295-018-00140-5.

[6] A. Jolley, G. Cohen, D. Joubert, A. Lambert, Evaluation of Event-Based Sensors for Satellite Material Characterisation, Journal of Spacecraft and Rockets, Vol. 59, pp. 627-636, 2022, https://doi.org/10.2514/1.A35015.

[7] G. Gallego, T. Delbruck, G. Orchard, C. Bartolozzi, B. Taba, A. Censi, S. Leutenegger, A. Davison, J. Conradt, K. Daniilidis, D. Scaramuzza, Event-Based Vision: A Survey, IEEE Transactions on Pattern Analysis and Machine Intelligence, IEEE, NewYork, July 2020, pp. 1–26. https://doi.org/10.1109/TPAMI.2020.3008413.

[8] C. Posch, D. Matolin, R. Wohlgenannt, A QVGA 143 dB Dynamic Range Frame-Free PWM Image Sensor with Lossless Pixel-Level Video Compression and Time-Domain CDS, Journal of Solid-State Circuits, Vol. 46, No. 1, 2011, pp. 259–275, https://doi.org/10.1109/JSSC.2010.2085952.

[9] T. Finateu, A. Niwa, D. Matolin, K. Tsuchimoto, A. Mascheroni, E. Reynaud, P. Mostafalu, F.T. Brady, L. Chotard, F. Legoff, H. Takahashi, H. Wakabayashi, Y. Oike, C. Posch, A 1280×720 Back-Illuminated Stacked Temporal Contrast Event-Based Vision Sensor with 4.86μm Pixels, 1.066GEPS Readout, Programmable Event-Rate Controller and Compressive Data-Formatting Pipeline, IEEE International Solid-State Circuits Conference, 2020, pp. 112-114.

[10] University of Bern, Astronomical Institute Zimmerwald Observatory, 2022, https://www.aiub.unibe.ch/research/zimmerwald_observatory/index_eng.html, (accessed 29 Aug 22).

[11] C. Peat, Heavens Above, 2022, https://heavens-above.com/, (accessed 06 Jul 22).

[12] J. Rodriguez-Villamizar, T. Schildknecht, Efficient and Robust Algorithms for the Real-Time Optical Tracking of Space Debris, Proc. 8th European Conference on Space Debris (virtual), Darmstadt, Germany, 20–23 April 2021.